university of groningen

faculty of science and engineering

The Effects of Dust Grain Surface Reactions on the HDO/H_2O Ice Ratio in Protoplanetary Disks

Author:
Tycho Hebels
(s4763130)

Supervisor:
prof. dr. Inga Kamp
Second examiner:
dr. Tim Lichtenberg

Bachelor's Thesis
To fulfill the requirements for the degree of
Bachelor of Science in Astronomy
at the University of Groningen

July 4, 2024

Abstract

The deuterium-to-hydrogen (D/H) ratio can vary substantially in protoplanetary disks due to radial drift, turbulence and vertical settling. Molecules and atoms are able to freeze out onto the surfaces of dust grains moving through the disk. This thesis looks at the surface chemistry happening in these icy mantles, particularly the reactions that might affect the D/H ratio of water ice. We investigate their timescales and reaction rates by utilizing the Stochastic Monomer Processor (SHAMPOO) and Protoplanetary Disk Model (ProDiMo) codes to simulate H_2O and HDO forming reactions at radial distances ranging from $10 - 60$ AU from the star. We find that surface reactions with low activation energies are able to enhance the D/H ratio of water ice by a factor of $\sim 2-5$ depending on distance and the initial D/H value. Temperatures are higher closer to the star, which causes higher reaction rates, but the impact on the D/H ratio of water ice is largest when the initial value is lowest, which in our simulations is at 60 AU. Our finding suggests that surface chemistry on dust grains is able to enhance the D/H ratio of water ice, even when going far out in the protoplanetary disk.

Contents

1 Introduction

The most common hydrogen isotope is deuterium, denoted as D. It consist of one neutron and one proton, making it slightly heavier than regular hydrogen. Most of it was formed during the Big Bang nucleosynthesis (Ryden, 2016), resulting in a specific amount of deuterium that has not significantly changed since then. This isotope can result in so-called deuterated species, such as HDO. The ratio between HDO and H_2O is dependent on the formation environment and can give us insight into how water was formed on Earth. It is therefore worth investigating this ratio during the early stages of the Solar System to learn more about the origins of water on Earth.
We will begin by looking at protoplanetary disks.

1.1 Formation of Protoplanetary Disks

Protoplanetary disks are rotating disks of gas with a protostar at its center. They are formed by molecular clouds that are dense and massive enough to collapse under their own gravity. A protostar will form at the center, with gas rotating around it as illustrated in 1. If the protostar has a mass greater than roughly 0.08 solar masses, the gravitational energy will be large enough such that hydrogen fusion can occur within the core due to the increased temperature (LeBlanc, 2010). These protostars are the first step in stellar evolution.

The remnants of gas from the collapsed cloud will continue to accrete towards and around the protostar, which starts to heat up. The gas cannot accrete directly onto the disk due to its angular momentum, creating a circumstellar disk around the protostar. This is where planet formation will eventually occur, with the disk itself lasting around $10^6 - 10^7$ years (Haisch et al., 2001). The disk can be divided into two regions by the water-snowline, the distance at which water ices can begin to form onto dust grains (shown on the left of Figure 2). The inner part of this line is where rocky planets are thought to form, while the outer region is home to gas giants.

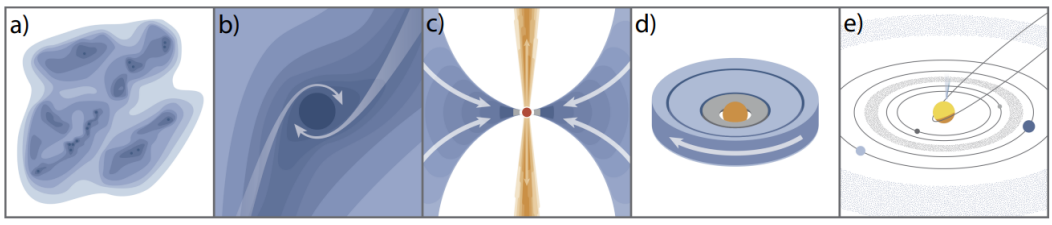

Figure 1: The evolution of a molecular cloud up until the formation of a planetary system. a) The molecular cloud slowly becomes massive and dense enough. b) The cloud collapses, creating a protostar at the center with the remaining gas spiraling around it. c) Some gas is ejected from the system while the rest begins to settle around the core. d) A circumstellar rotating circumstellar disk is formed. e) A planetary system is formed. Credit: Öberg & Bergin (2021)

1.2 Circumstellar Disk Processes

Dust grains move throughout the protoplanetary disk both radially and vertically. Three main mixing processes will be discussed: radial drift, vertical settling and turbulent diffusion, all of which are also shown in Figure 2.

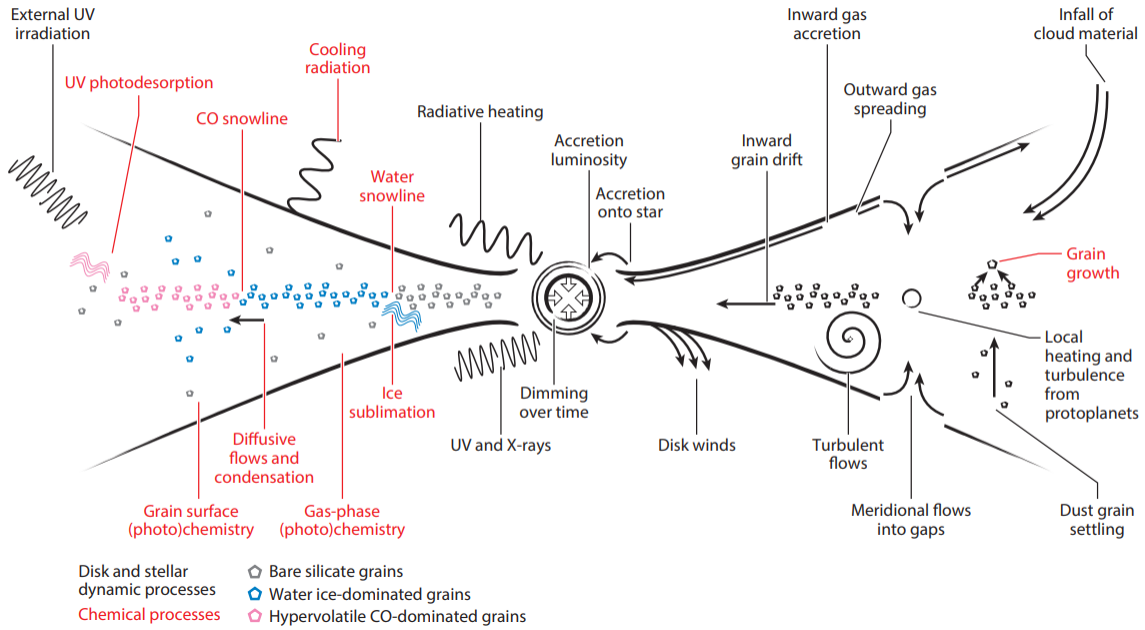

Figure 2: Overview of many dynamical and chemical processes present within a protoplanetary disk, denoted by black and red respectively. Notable processes are radial drift, turbulent diffusion and vertical settling, shown on the right side of the figure, describing how a dust particle moves throughout the disk. These processes are discussed in Section 1.2 in more detail. Credit: Öberg et al. (2023)

The first type of transport that can occur within a disk is radial drift. Gas inside of a disk moves at a velocity that is slightly sub-Keplerian due to a pressure gradient (Weidenschilling, 1977). Drag forces can then cause particles to experience a headwind whose strength depends on their size and density, resulting in a loss of angular momentum. This then causes the particles to drift radially. Particles can either move with the gas; move with velocities much smaller than the gas; or move with velocities much larger than the gas depending on their size and density (Stepinski & Valageas, 1996, 1997). These regimes are determined by Stokes number. Most particles inside disks are transported inwards, though some outward transport is possible by local reversals in the pressure gradient (Whipple, 1973).

Another effect is vertical settling. Particles are attracted by the vertical component of the gravitational force of the protostar and slowly move towards the midplane, which causes a higher dust density. All intermediate-sized particles ($10^1 - 10^{-4}$ cm) settle to the midplane on timescales of a few hundred years, while very large particles show oscillations about the midplane (Garaud et al., 2004; Barrière-Fouchet et al., 2005).

Turbulent diffusion stirs dust particles up to higher regions of the disk. This can counteract vertical settling by some amount, but gravity eventually dominates given enough time.

Besides these transport and mixing processes, micrometer sized dust particles can begin to collide and form aggregates: a collection of dust particles being loosely bound together. These aggregates can continue to interact with each other through collisions, undergoing coagulation (Dominik & Tielens, 1997) and fragmentation (Gunkelmann et al., 2016). An aggregate can therefore grow and shrink as it travels through the disk.

When a particle is beyond the snowline, atoms and molecules from the gas phase can stick onto its surface and create an ice layer (shown on the left side of Figure 2). Water is the most prominent ice component found on dust grains. Chemical reactions can then proceed to take place within these ice mantles.

1.3 Deuterium

Deuterium was formed during the Big Bang nucleosynthesis. This is where protons and neutrons fused together under extreme conditions to form elements heavier than hydrogen. The binding energy of deuterium is about 1.6×10^5 larger than the ionization energy of hydrogen (Ryden, 2016), which tells us that deuterium was formed at much higher temperatures. Once the Big Bang nucleosynthesis phase was over and everything cooled down enough, the amount hydrogen and deuterium was fixed, with D/H being the deuterium abundance. This is something we can both calculate from the binding and ionization energy fraction mentioned before, and from observations, with the most recent value having been estimated to be $2.0 \pm 0.1 \times 10^{-5}$ by Friedman et al. (2023).

Though this value stays mostly constant throughout the interstellar medium, it can change depending on the environment. Figure 3 shows some singular solar objects with their D/H ratio. Inside of protoplanetary disks, values of the D/H ratio can vary substantially. Deuterium

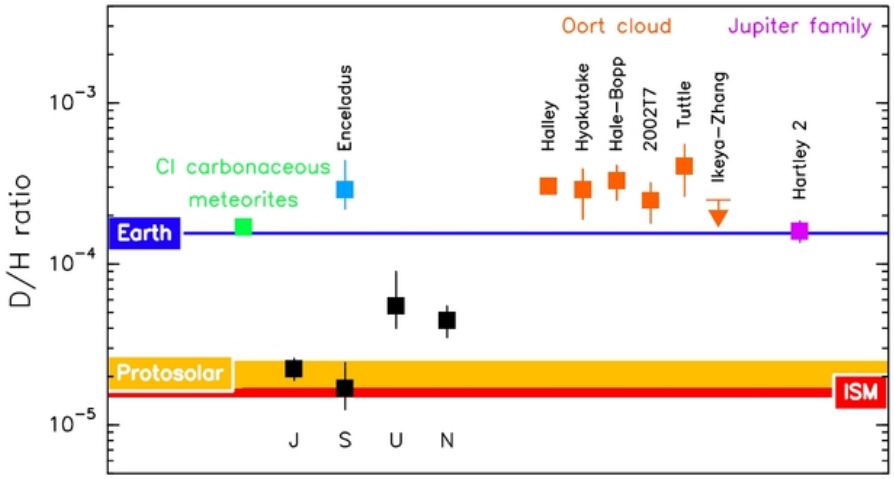

Figure 3: D/H ratio's of various solar objects. The orange points are six comets residing within the Oort cloud. The outer most planets are also shown below (Jupiter, Saturn, Uranus and Neptune respectively) in black, as well as Saturn's moon and CI chondrites just above. Credit: ESA Herschel (Paul Hartogh)

can get enriched or depleted due to the mixing processes present in the disk and chemical fractionation in cold environments. Furuya et al. (2013), for example, looked into the effects of turbulent mixing and found that the HDO/H_2O ice ratio can change as much as a factor of 10^2 when cycling through the vertical layers of the disk. They did this by investigating vertical mixing due to turbulence carrying icy dust grains into higher regions of the disk, but they did not include radial drift of icy grains or collisions in their models.

1.4 Thesis Outline

The research questions we aim to answer in this thesis are as follows:

- How does the timescale of deuteration surface reactions compare to the dynamical timescales of dust grains?
- Does surface chemistry on dust grains have a significant impact on the HDO/H_2O ice ratio in the 10 - 60 AU region of a typical T-Tauri star protoplanetary disk?

Chapter 2 will give a review of surface chemistry and deuteration. Chapter 3 will explain the different models used to perform protoplanetary disk simulations. Chapter 4 will showcase the obtained results. Chapter 5 will discuss these results and some limiting factors to the simulations done. Lastly, Chapter 6 will conclude this research by giving a brief summary and suggesting what can be investigated further.

2 Surface Chemistry

Throughout this thesis, a lot of processes involve the surfaces of grains that move throughout a protoplanetary disk and their interactions with the surrounding gas. Here we will look at a few important aspects of such processes. I will closely follow the concepts described in Rocha et al. (2023) and Cuppen (2017).

2.1 Adsorption and Desorption

When particles from either a gas or liquid fall upon a surface and stick to it, we speak of adsorption. This sticking of particles to the surface through this process is similarly called adhesion. The atom or molecule is called the adsorbate and the surface it sticks to the adsorbent. The amount of energy lost in order to make this process possible is referred to as the adsorption energy (E_{ads}). In the case of this research, where we are looking at a protoplanetary disk, different molecules can adsorb onto the surface of a dust grain. A few relevant species and their adsorption energies are shown in Table 1. The reason for adsorption to happen has to do with the energy of the particle: upon contact, it loses some energy to the dust grain itself. If the remaining energy of the particle is not enough to break away from the dust grain again, the energy will slowly dissipate over time until thermal equilibrium is achieved.

There are a couple different ways in which an adsorbed particle can regain energy: thermal heating, incoming photon radiation or energetic electrons. Once the adsorbed particle has gained enough energy to overcome the binding energy onto the grain's surface, it will desorb and the particle is released. In our case, photons are the primary process of desorption and it is referred to as photodesorption.

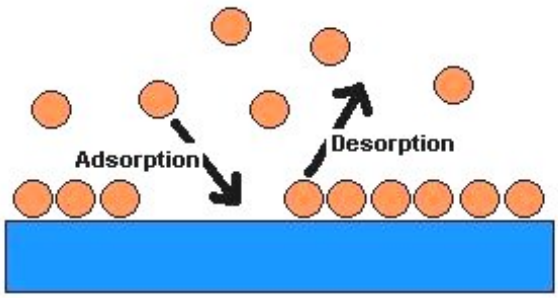

Figure 4: An illustration of adsorption and desorption. Particles fall onto the surface and stick to it, before getting released again upon gaining enough energy. Credit: `https://www.chemieunterricht.de/dc2/chromato/adsorpdef.htm`

2.2 Reactions

Grain surfaces inside of the protoplanetary disk can undergo two different types of reactions: Eley Rideal and Langmuir-Hinshelwood type reactions. The former involves only one molecule being adsorbed and reacting directly with a molecule that is in the gas phase. However, since we are mainly focusing on what happens directly on the surface itself, the latter reaction type

Species	E_{ads} (K)	Mass (u)	Reference
H	600	1	A
D	621	2	E
H_2	430	2	B
D_2	430	4	F
O	630	16	D
OH	1000	17	B
OD	1000	18	F
H_2O	4800	18	C
HDO	4800	19	F

Table 1: Adsorption energies and mass of relevant species. References: Cazaux & Tielens (2002) (A), Garrod & Herbst (2006) (B), Brown & Bolina (2007) (C), Aikawa & Herbst (1999) (D) and Caselli et al. (2002) (E). D_2, OD and HDO are kept the same as their non-deuterated variants, following Furuya et al. (2013) (F).

is required. This mechanism is the recombination of two molecules that diffuse and meet each other on the grain's surface. If we were to have two species named A and B, the Langmuir-Hinshelwood reaction would be as follows:

$$\mathrm{A\#} + \mathrm{B\#} \rightarrow \mathrm{AB\#}. \tag{1}$$

Here, the hashtag indicates that these species are bound to the surface. In order for the molecules to diffuse on the surface, they need to have enough energy to overcome the diffusion barrier. This can usually be achieved in two different ways.

1. The thermal energy is larger than the barrier energy, allowing the molecules to freely move along the surface and react with each other.

2. The thermal energy is lower than the barrier energy. In this scenario, the molecule will either jump over the energy barrier by gaining some thermal energy or get through the boundary by quantum tunneling.

Both of these are mechanisms are called hopping, with the former being a classical form of hopping and the latter being a quantum one. How quickly and efficiently a molecule diffuses over the surface will depend on the amount of time it takes to overcome the diffusion barrier, called the hopping time

$$\tau_{\mathrm{hop},i} = \frac{e^{f \cdot E_{\mathrm{ads},i}/k_B T_d}}{\nu_i^{\mathrm{osc}}} \ \mathrm{s}, \tag{2}$$

where ν_i^{osc} is the lattice vibration of the molecule described as

$$\nu_i^{\mathrm{osc}} = \sqrt{\frac{2 N_{\mathrm{surf}} \cdot f \cdot E_{ads,i}}{\pi^2 m_i}} \ \mathrm{s}^{-1}, \tag{3}$$

where N_{surf} is the surface binding site density given as 1.5×10^{15} cm^{-2} (Rocha et al., 2023). T_d is the dust temperature in K, k_B is the Boltzmann constant in erg K^{-1}, m is the molecule mass in g and E_{ads} is the adsorption energy in erg, with the height of the diffusion barrier being a

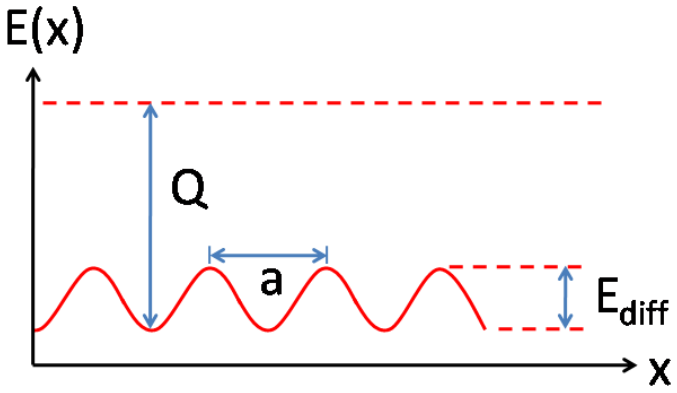

Figure 5: A depiction of surface diffusion. Q is the thermal energy, a is the barrier width and E_{diff} is the barrier height. The dotted line showcases scenario 1 where there is free diffusion. If this line were somewhere between E_{diff}, scenario 2 would play out where the molecule would either have to a), hop over the barrier by gaining thermal energy or b), quantum tunnel through. Credit: `https://en.wikipedia.org/wiki/Surface_diffusion`

fraction of this value, i.e. $f \cdot E_{\text{ads}}$. It is important to note that the precise value of f is not known. Values between 0.3 and 0.8 are often chosen when modelling these types of surface reactions. For this research we have chosen $f = 0.33$, following the estimated value of water ice as given in Cuppen (2017). The diffusion rate is then given by

$$R_i^{\text{diff}} = \frac{1}{\tau_{\text{hop},i} \cdot N_{\text{site},i}} \text{ s}^{-1}, \tag{4}$$

where N_{site} is the amount of binding sites (or diffusion barriers) present on the surface. Assuming a spherical particle, this becomes

$$N_{\text{site}} = 4\pi a^2 N_{\text{surf}}, \tag{5}$$

where a is the particle radius in cm. The total diffusion rate between two molecules over a surface will then be

$$R^{\text{diff}} = \begin{cases} (R_i^{\text{diff}} + R_j^{\text{diff}}) N_j \text{ s}^{-1} & \text{if } N_i \geq Nj \\ (R_i^{\text{diff}} + R_j^{\text{diff}}) N_i \text{ s}^{-1} & \text{if } N_i < Nj \end{cases} \tag{6}$$

where N is the total amount of a given species present on the surface. Whether N_i or N_j is chosen depends on which is less abundant.

Before the diffused molecules are able to react with each other, they need to overcome a reaction barrier, which is termed the activation energy. This can either be done by thermally hopping over it like described earlier, or quantum tunnelling. Bell's formula is used to determine the probability of overcoming such a barrier between two molecules, where both classical and quantum effects are taken into account,

$$Q_{\text{Bell}} = \frac{\beta^{-\alpha} - \alpha^{-\beta}}{\alpha - \beta}, \tag{7}$$

where α and β are parameters defined as:

$$\alpha = \frac{E_{\text{act}}}{k_B T_g} \tag{8}$$

and

$$\beta = \frac{4\pi a_i}{h}\sqrt{2\mu E_{\rm act}}. \tag{9}$$

Here, $E_{\rm act}$ is the height of the activation energy barrier for a given reaction to happen in erg, a_i is the width of the activation energy barrier in cm, h is the Planck constant in erg s and T_g is the gas temperature in K. Lastly, μ is the reduced mass of the two molecules, given by

$$\mu = \frac{m_i m_j}{m_i + m_j}\ \text{g}. \tag{10}$$

The probability P of overcoming the reaction barrier is then given by

$$P = \frac{Q_{\rm Bell}}{Q_{\rm Bell} + w_i^{\rm diff} + w_j^{\rm diff}}, \tag{11}$$

where

$$w_i^{\rm diff} = \frac{R_i^{\rm diff} N_{\rm site}}{\nu_i^{\rm osc}}. \tag{12}$$

The total amount of reactions happening each second on a surface between two molecules is then simply

$$R = R^{\rm diff} \cdot P\ \text{s}^{-1}. \tag{13}$$

2.3 Deuteration

The formation of HDO and H_2O ice on the surfaces of grains can happen through the following reactions:

$$\text{O\#} + \text{D\#} \rightarrow \text{OD\#} \tag{14}$$

$$\text{O\#} + \text{H\#} \rightarrow \text{OH\#} \tag{15}$$

$$\text{OD\#} + \text{H\#} \rightarrow \text{HDO\#} \tag{16}$$

$$\text{OH\#} + \text{D\#} \rightarrow \text{HDO\#} \tag{17}$$

$$\text{OH\#} + \text{H\#} \rightarrow \text{H}_2\text{O\#} \tag{18}$$

Figure 6 shows the different formation pathways of these reactions. Only regular hydrogen species are shown here, but the same pathways apply for the deuterated species. All of these reactions have an activation energy of zero, which means the reaction can happen freely. Consequently, the probability in Equations 11 and 13 reduce to one. Only the mass and adsorption energy (shown in Table 1) of each molecule or atom will therefore determine the reaction rate. Once water and deuterated water have formed, they can continue to react with each via:

$$\text{H2O\#} + \text{OD\#} \rightarrow \text{HDO\#} + \text{OH\#} \tag{19}$$

$$\text{HDO\#} + \text{OH\#} \rightarrow \text{H2O\#} + \text{OD\#} \tag{20}$$

Equation 19 has an activation energy of 2078 K (Masgrau et al., 1999) while the reverse reaction has an activation energy of 3165 K (Masgrau et al., 1999), meaning the formation of HDO is favored.

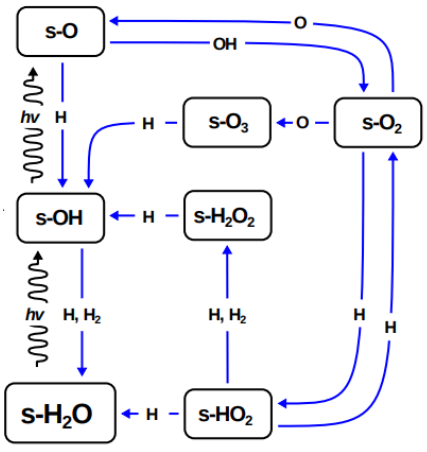

Figure 6: Illustration of the different formation pathways of water ice on the surfaces of dust grains. Credit: M. Persson, based on van Dishoeck et al. (2011, 2013).

3 Modelling

We will use two codes to simulate the dust grain movement and protoplanetary disk background, those being the Stochastic Monomer Processor (SHAMPOO) (Oosterloo et al., 2023) and ProDiMo (Thi et al., 2011, 2013; Kamp et al., 2010; Woitke et al., 2009) respectively.

3.1 Stochastic Monomer Processor

The SHAMPOO code simulates the full coupling of dynamical transport, collisional processes and ice processes (discussed in Chapter 1.2) of a so-called monomer. This acts as a tracer particle which is placed within an aggregate inside of a protoplanetary disk environment, shown in Figure 7. The monomer itself is assumed to be spherical, with mass m_m and radius $s_m = 5 \cdot 10^{-8}$ m, while the aggregate has an effective radius of s_a which changes due to collisional coagulation and fragmentation. These processes also cause the tracing monomer to become embedded within other aggregates upon collisions. Therefore, the aggregate where the monomer is residing in throughout the simulation is referred to as the home aggregate.

The depth of the monomer inside its home aggregate is defined as z_m and determines the adsorption efficiency onto the monomer, as well as the photodesorption. When molecules and photons from outside the aggregate are able to reach the monomer, it is considered to be exposed. This is determined via a probability function. The critical monomer depth is defined as the point where the distance between the aggregate surface and the monomer itself is that of the monomer's diameter, i.e, $z_{crit} = 2s_m$. This ensures that monomers that get close enough to the surface of the aggregate are always exposed regardless of the probability function.

The simulation itself spans 100 kyr and has a maximum radius of 100 AU from the host star, which is determined from the disk background model (Section 3.2). Anything beyond this limit will yield unreliable results (Oosterloo et al., 2023). An input file is used to set all the previously mentioned values, as well as which of the physical processes are included in the simulation. Either the radial or vertical position of the monomer can also be fixed in place. A more detailed description about SHAMPOO's inner workings can be found in Oosterloo et al. (2023).

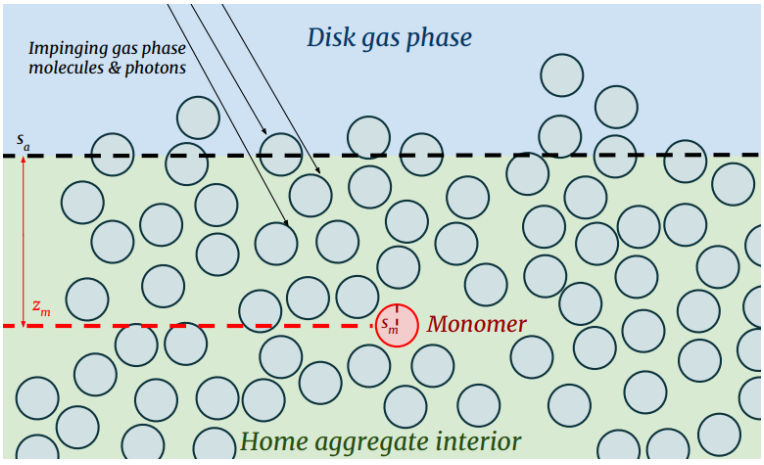

Figure 7: An illustration of the monomer embedded inside of its home aggregate. Credit: Oosterloo et al. (2023)

3.2 Protoplanetary Disk Model

SHAMPOO needs information about the local environment where the monomer and aggregates move in. Important are the gas and dust densities, temperatures, and the number densities of all the species the code tracks. This is done with the theoretical disk model ProDiMo, which calculates the chemical composition and physical quantities of each point in a grid which covers the protoplanetary disks radial and vertical dimensions. SHAMPOO uses these values and updates the monomer about its surroundings for each time step during the simulation.
The disk model surrounds a typical T-Tauri star. The key parameters for both the protostar and the disk itself are shown in Table 2.

Parameter	Name	Value	Units	Reference
M_*	Stellar mass	0.7	$M_\odot$	A
L_*	Stellar luminosity	6	$L_\odot$	B
T_{eff}	Effective temperature	4000	K	B
M_{disk}	Disk mass	0.1	$M_\odot$	C
r_{in}	Inner disk radius	0.07	AU	A
r_{out}	Outer disk radius	600	AU	C

Table 2: Input parameters for ProDiMo. References: Woitke et al. (2016) (A), Siess et al. (2000) (B) and Oosterloo et al. (2023) (C)

Figure 8 shows the 2D distributions of the gas and dust temperature, the gas density and the HDO/H_2O ice ratio of the disk. From the first two plots we can conclude that in most of the $10 - 60$ AU regime, the gas and dust temperature are equal.

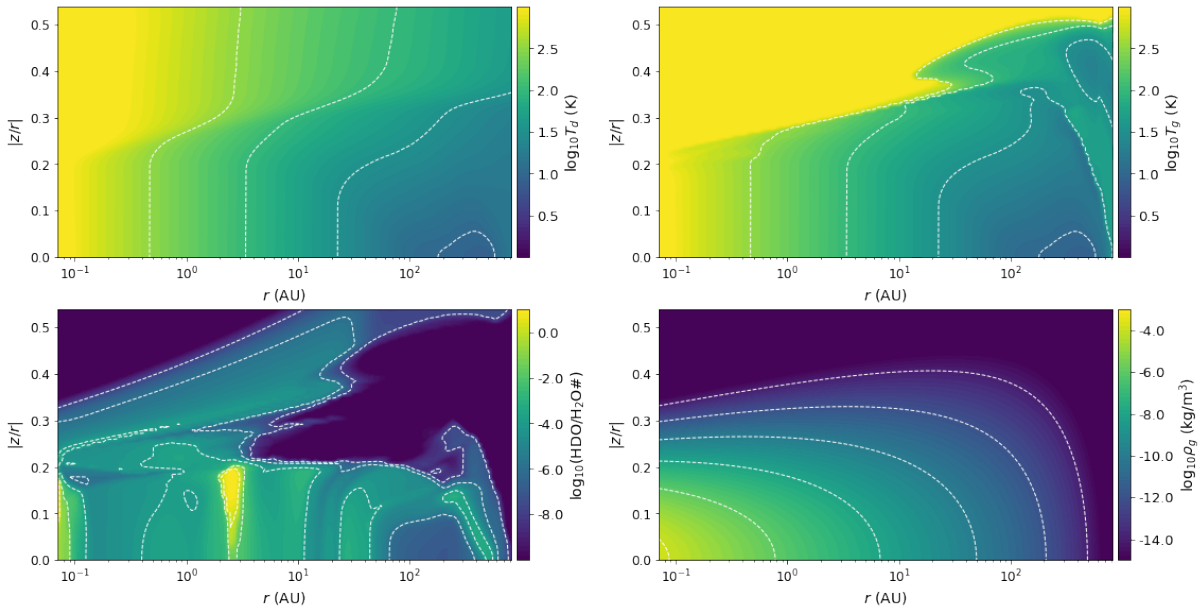

Figure 8: Protoplanetary disk temperature profile (upper left and right) of both dust and gas, HDO/H_2O ice ratio (lower left) and gas density profile (lower right) taken from the background model. The x-axis shows the radial distance from the center of the disk in AU, while the y-axis shows the z/r aspect ratio.

3.3 Approach

We will develop a code that calculates the reaction rate and all relevant parameters from Chapter 2.2 for the formation reactions of H_2O and HDO ice using SHAMPOO and ProDiMo. Shown in Figure 9 is an example of the SHAMPOO code. The monomer is let loose at a radial

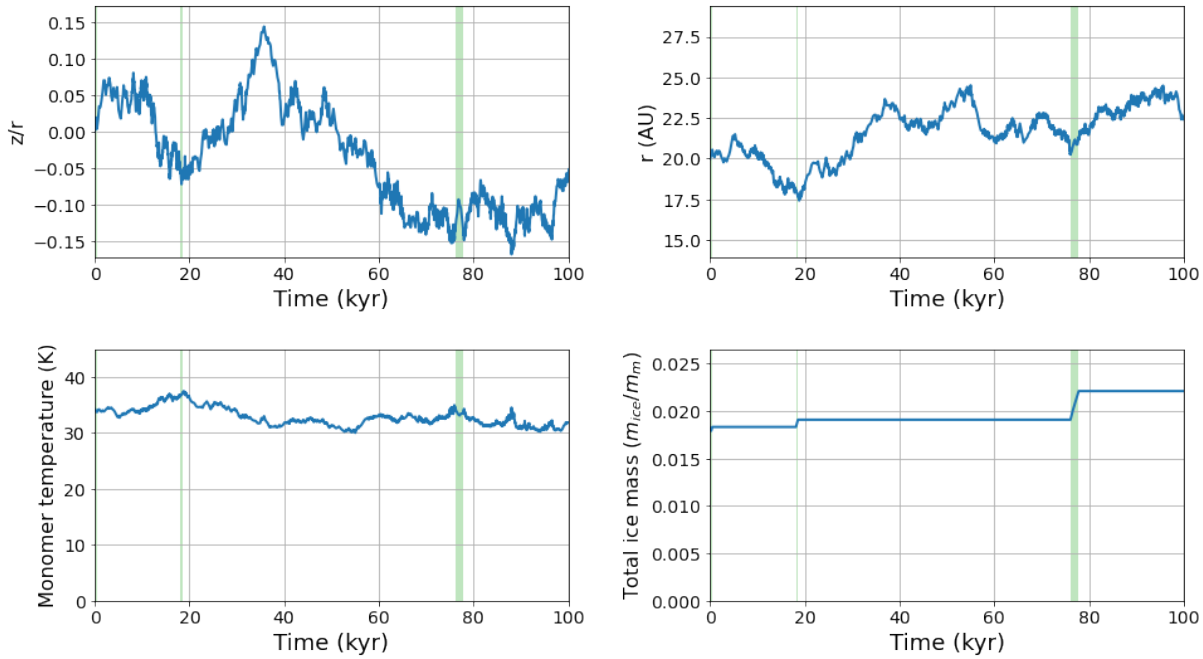

Figure 9: Outputs of a run at r = 20 AU. We have the z/r distance (upper left), radial distance (upper right), temperature (bottom left) and total ice mass (bottom right) as a function of time. The green areas are sections where the monomer is exposed outside of the aggregate.

distance of 20 AU from the star. It will then freely move throughout the disk for 100 kyr while undergoing radial drift, vertical settling, turbulent diffusion and collisions. Values for the dust temperate T_d, the ice mass m_{ice} and amount of atoms or molecules N in the ice mantle of any given species are taken from SHAMPOO, while the mass m, adsorption energy E_{ads} and activation energy E_{act} are taken from ProDiMo.

We then compute the reaction rate from Equation 13 of reactions 16, 17, 18, 19 and 20, while looking specifically at the regions between exposures (green areas). During exposures, lots of species will be able to adsorb onto the monomer's surface. Since SHAMPOO does not contain a chemical network, species are not depleted when reacting with each other. This causes the total amount of any given species N in Equation 6 to be extremely large, resulting in an unrealistically high reaction rate.

Reactions 16 and 17 presents HDO ice to the monomer, and reaction 18 is adds H_2O ice, both of which are already on the monomer. We assume that the hydrogen atoms will distribute themselves evenly into reactions 16 and 17. This will enhance the HDO/H_2O ice ratio ice by a certain amount together with the exchange reactions 19 and 20. The resulting HDO/H_2O ice ratio is then compared to the one taken directly from SHAMPOO, where no surface chemistry is considered.

We conduct 10 runs at distances ranging from 10 to 60 AU, taking averages of the exposure frequency, total exposure time and reaction rate for each reaction. This allows us to calculate, on average, how long a monomer stays in its home aggregate before being exposed. An assumption is made here that the exposure times are evenly spaced out when considering multiple runs. The reaction rate is then integrated over this time interval to get the total amount of surface reactions that have taken place.

4 Results

4.1 Timescales of Physical and Chemical Processes

Dynamical processes, collisional processes and adsorption and desorption all have their own typical timescales. Comparing these with each other can give insight as to where the corresponding processes are dominating or coupled. Oosterloo et al. (2023) gives an overview of the various timescales, but we will additionally consider the overall ice evolution on the monomer which includes the above mentioned processes. The change in ice is calculated by taking the difference of two adjacent mass values and dividing by the associated timestep value,

$$\frac{\partial M}{\partial t} = \frac{M_i(t_{n+1}) - M_i(t_n)}{\Delta t_n}. \tag{21}$$

The typical ice evolution timescale τ_{ice} is then calculated as

$$\tau_{\text{ice}} = |\frac{M_i(t_n)}{\frac{\partial M}{\partial t}}|. \tag{22}$$

Equation 21 can either be positive or negative, which implies a mass gain or loss respectively. We want to determine the overall change of the ice mantle, hence the absolute value is taken. The chemical timescale of any given reaction between two species is simply given by taking the inverse of the reaction rate given by Equation 13,

$$\tau_{\text{chem}} = \frac{1}{R}. \tag{23}$$

Figure 10 compares the various timescales over the 100 kyr simulation and the evolution of the ice mass. We can see that the ice mass only changes when the associated timescale is smaller than 100 kyr, indicated by the dashed line. This is also where the monomer is exposed to the surrounding gas, indicated by the green areas. The chemical timescales remain below the $t = 10^5$ yr line, with some notable dips when the monomer is exposed.

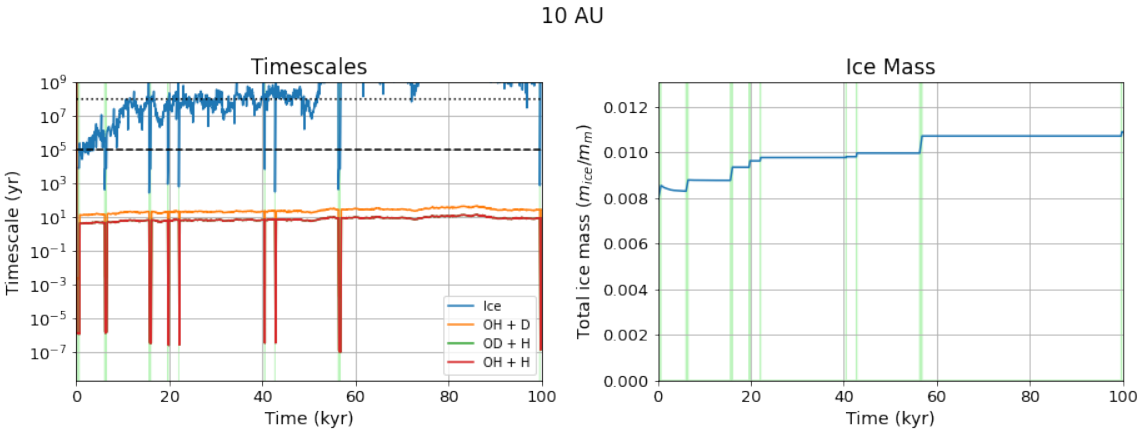

Figure 10: Timescale (left) and ice mass (right) evolution at a distance of 10 AU from the center of the disk. The ice mass is shown as a fraction of the total monomer mass. The dashed line at $t = 10^5$ yr indicates the time of the simulation itself. The dotted line at $t = 10^8$ yr is the upper limit of relevant timescales for planet formation. The green areas are sections where the monomer is exposed outside the aggregate.

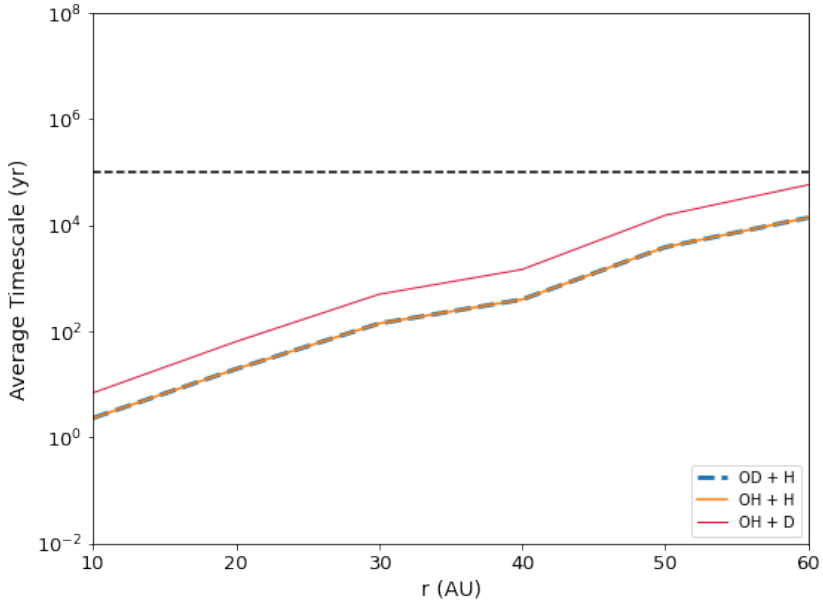

Figure 11: Timescales of the relevant reactions as a function of radial distance. The dashed line indicates $t = 10^5$, the duration of the simulation.

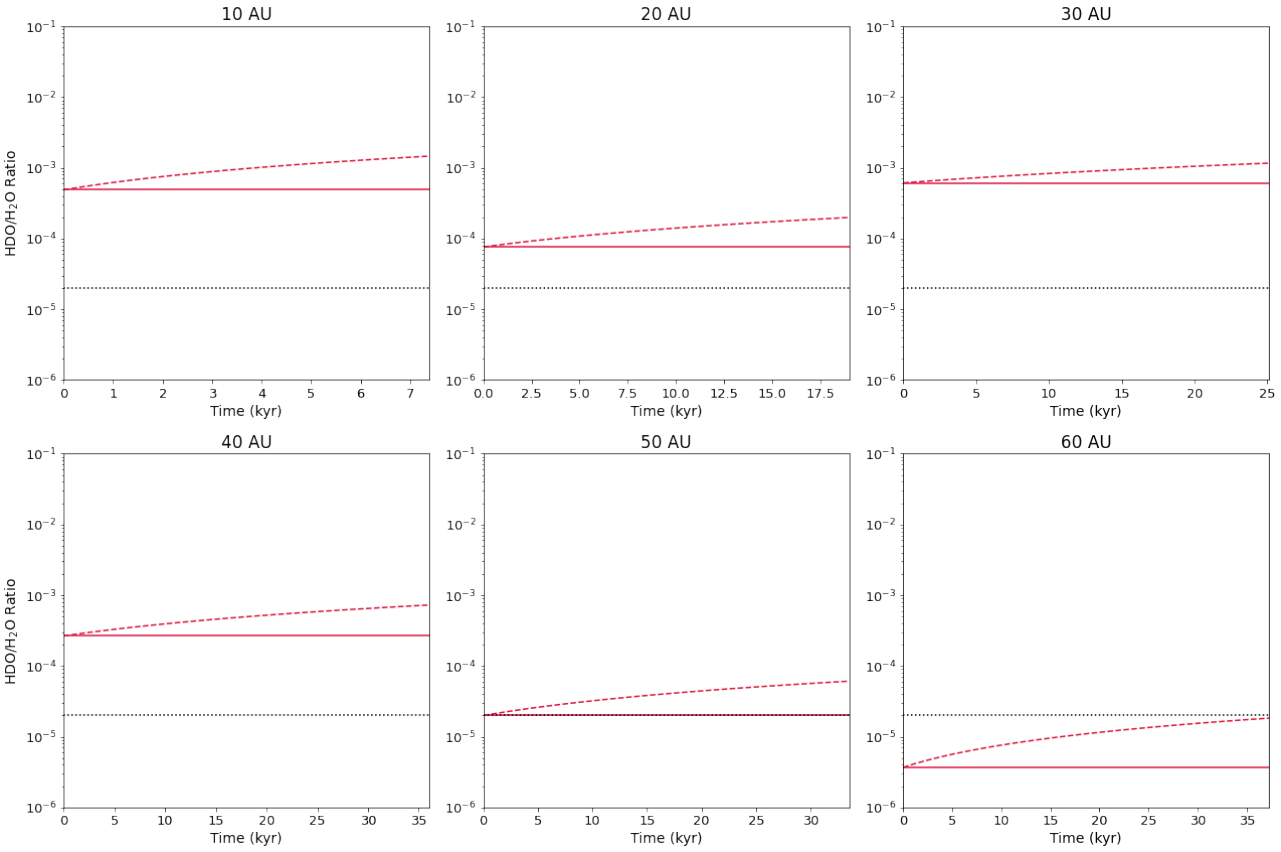

Figure 12: Enhancement of the HDO/H_2O ice ratio due to surface grain reactions over time. The solid line is the regular HDO/H_2O ice ratio taken directly from SHAMPOO, while the dashed line shows the increase over time. The black dotted line denotes 2×10^{-5}, the D/H value of the interstellar medium.

4.2 Chemical Timescales

Figure 11 shows the chemical timescale τ_{chem} of each reaction as a function of radial distance, with the dashed line at $t = 10^5$ yr indicating the duration of the simulation. The timescales are calculated from Equation 23, where the average reaction rate of all 10 runs at each distance is used. Reactions 17 and 18 appear to have identical timescales, while reaction 16 is larger by a factor of $\sim 3 - 4$, increasing with distance. The timescales for all reactions start to increase as we go further out into the disk, but they all remain under the $t = 10^5$ yr line. Reactions 19 and 20 do not appear in the plot since their timescales are much greater than 10^9 yr.

4.3 HDO/H_2O Ratio on Grains

The enhancement of the HDO/H_2O ice ratio over time for each distance is shown in Figure 12. The solid line is the HDO/H_2O ice ratio taken directly from SHAMPOO, while the dashed line shows how much this ratio gets enhanced due to the reactions happening on the surface of the monomer. The initial HDO/H_2O ice ratio taken from SHAMPOO also varies between distances.

The maximum amount of enhancement due to surface reactions happens at 60 AU, seen in Figure 12, where the HDO/H_2O ice ratio is increased from 3.7×10^{-6} to 1.8×10^{-5}. The final value is a factor of ~ 5 higher. The initial ratio at this distance is also the lowest when compared to all other distances.
At 30 AU, surface reactions have the least amount of impact on the HDO/H_2O ice ratio. It is increased from 6.1×10^{-4} to 1.1×10^{-3}, a factor of ~ 2 higher. This is also where the initial value is the highest out of all distances.

5 Discussion

The dips in Figure 10 are a result of the monomer being exposed to the surrounding gas. Species present in the gas phase that have high number densities will adsorb onto the surface rapidly. Figure 13 shows these number densities for H_2O, HDO, OH, OD, H and D, with the latter two being notably high in the $10 - 60$ AU region. This then causes reactions 16, 17 and 18 to occur at an unrealistically high rate due to chemistry not being considered in SHAMPOO.
We also see that reactions 20 and 19 are not present in Figures 10 and 11. These reactions have an activation energy of 2078 K and 3165 K respectively, which causes them to be on timescales greater than 10^9 yr. The typical timescales of disks are on the order of $10^6 - 10^7$ yr, implying that these high activation energy reactions are negligible when looking at surface reactions.

All other considered reactions have no activation energy, allowing their rates to be much higher. Figure 11 shows how these reactions are able to happen up until a distance of 60 AU. The reason for reactions 17 and 18 having the exact same timescales is their adsorption energy (Table 1). OD and OH share the same adsorption energy, meaning the only differing factor is the slightly higher mass of deuterium. Reaction 16, shown in red, is shifted up because of deuterium's adsorption energy being 21 K higher than hydrogen.

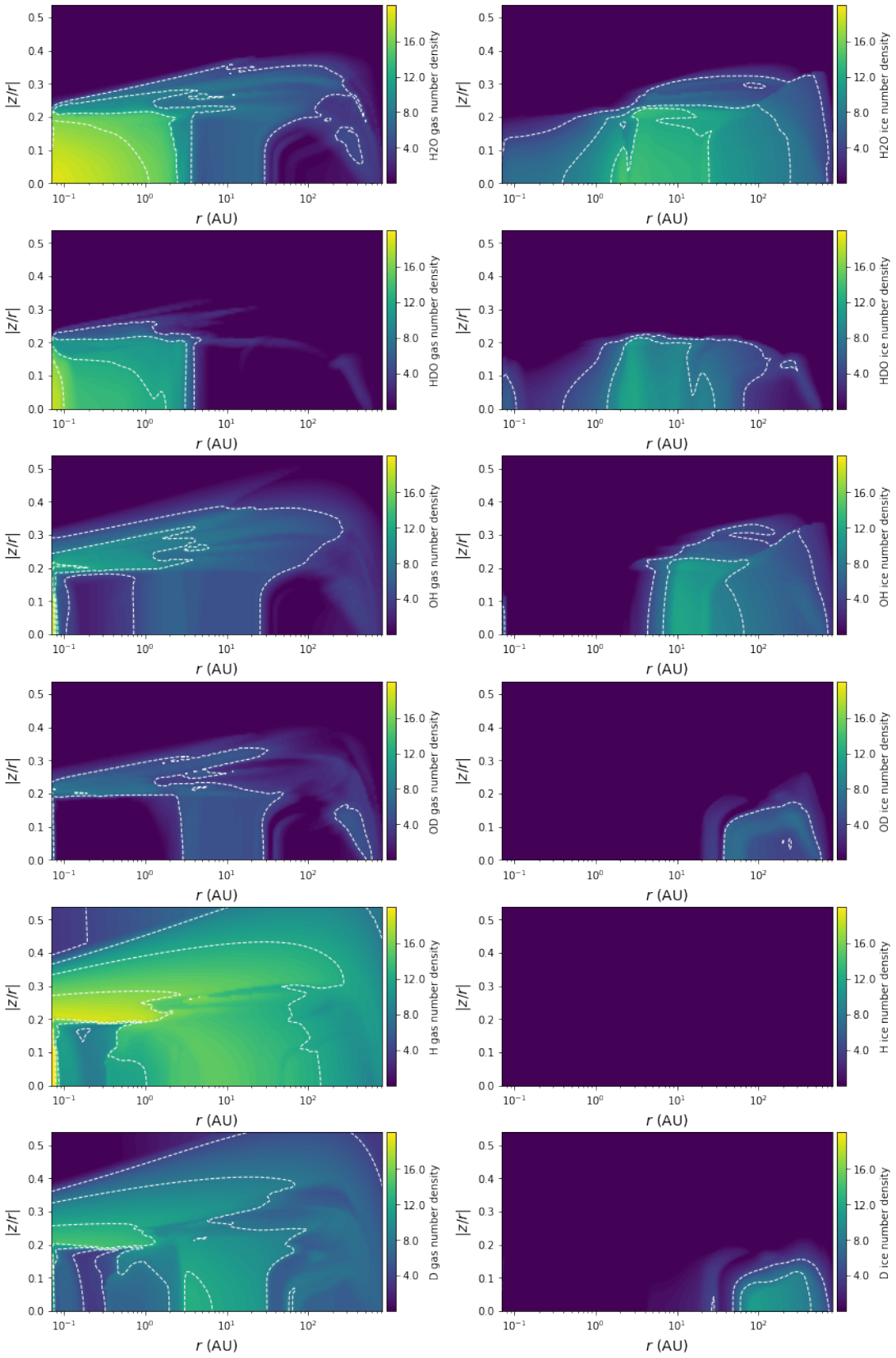

Figure 13: Gas and ice number densities of important species. The x-axis shows the radial distance from the center of the disk in AU. The y-axis shows the z/r ratio.

The increase in the HDO/H_2O ice ratio shown in Figure 12 depends on a few different variables. Firstly, the amount of time shown on the x-axis is not the same for every distance. The monomer is exposed to the surrounding gas more frequently when closer to the star. This causes the average amount of time for surface reactions to take place to be relatively low, increasing as we go to farther distances where there are less exposures.

Adsorption energy, mass and dust temperature all determine the reaction rate, but only the latter changes as the monomer moves through the disk. Figure 9 shows the dust temperature on the upper left side. There is a fairly simple relation: the closer we are to the star, the higher the temperature. Subsequently, the reaction rates will be highest at distances close to the star, decreasing as we move away in the disk.

Another important factor is the initial HDO/H_2O ice ratio taken directly from SHAMPOO. The lower left side of Figure 9 shows the HDO/H_2O ice ratio of the background disk model that is used. We see that between $10 - 20$ AU, values decrease and increase again slightly. From around $r > 40$ AU, we enter a region where the values become significantly smaller. We see this reflected in Figure 3 where the initial HDO/H_2O ice ratio value is lowest at 60 AU, which is also where the biggest increase happens. It appears that the total amount of enhancement done by surface reactions is most dependent on this initial value. Reaction rates are much higher at 30 AU due compared to farther distances due to higher temperatures, yet the impact on the HDO/H_2O ice ratio is much less.

Furuya et al. (2013) has shown that turbulent vertical mixing can decrease the D/H ratio of water ice. They found that turbulence stirs water to the upper regions of the disk before destroying it by photoreactions, producing atomic oxygen which is then transported back to the midplane where it reforms into water and other molecules. At r $\sim 20 - 30$ AU, dust temperatures are too high to form OH radicals on grain surfaces. This caused the cycle to decrease the HDO/H_2O ice ratio from $\sim 2 \times 10^{-2}$ to $10^{-4} - 10^{-3}$. Our findings suggest that the inclusion of surface reactions on grains could increase these values again by a factor of ~ 5.

5.1 Limitations

SHAMPOO does not contain a chemical network for reactions within the ice. This led to the accumulation of HDO due to not depleting any H or D species inside of the ice mantle when the relevant reactions took place. In reality, these species would slowly deplete and alter the composition of the ice mantle. Species could also react into other molecules via different pathways not included in this study. This is why our results show a theoretical maximum, where all species react into the desired outcomes and no species are lost after reacting. The more realistic values would therefore be lower, but we can not say with confidence how much that would be. A chemical model would need to be implemented into SHAMPOO in order to investigate this.

ProDiMo uses some adsorption energies that are outdated, the most important one being OH and subsequently OD, since they are assumed to be the same. Ruffle & Herbst (2000) used a value of $E_{\text{ads}} = 1260$ K, while Garrod et al. (2008) used an even higher value of $E_{\text{ads}} = 2850$ K. This was only figured out near the end of this research, and since a background model was already constructed with all relevant deuterated species that used these older adsorption energies, we chose to stick with these values. Using the updated values might have a notable

difference on the results. As mentioned before and shown in Figures 10 and 11, the reaction OH + H and OD + H are virtually the same due to their adsorption energies. These higher adsorption energies would decrease the reaction rate, leading to higher timescales. The 21 K increase in adsorption energy of D compared to H already shows a noticeable increase by a factor of $\sim 3-4$ in Figure 11. Thus, if the energy for OH is increased by a large amount it could result in all reactions being on timescales larger than 10^5 yr.

There is also a limitation with how far out from the disk we can run experiments in SHAMPOO. When a monomer is placed far away, adsorption during exposures can become very efficient. This can ultimately result in the ice mantle growing incredibly large, sometimes up to the order of $m_{\rm ice}/m_{\rm m} \sim 10^6$, which is a nonphysical result. The amount of molecules present in such a large ice mantle would also drastically increase the effect described in Section 4.1, where too many reactions will take place due amount of molecules present.
Likewise, desorption of non-exposed monomers also becomes very efficient which causes the ice mantle to shrink rapidly. A large sample size of monomers needs to be considered in order to average out these two effects; the 10 simulations done at each distance for this thesis are not sufficient.

6 Conclusion

In this thesis we have looked at the relevance of dust grain surface reactions in a protoplanetary disk and how they might affect the HDO/H_2O ice ratio when dynamical and collisional processes are taken into account. A background model of the protoplanetary disk containing the deuterated species D, OD and HDO was created using ProDiMo. We then used SHAMPOO to track a monomer embedded in an aggregate and calculated the rates of HDO and H_2O ice forming reactions, as well as their timescales. We compared these to the ice mantle evolution. This was done for multiple radial distances from the star, ranging from $10-60$ AU. We used 10 simulations per distance to obtain our results. Our conclusion is as follows:

1. From $10 \leq$ r ≤ 60 AU, the timescales of low activation energy reactions are dominating when compared to all other processes. Surface chemistry should be included into SHAMPOO to more accurately display how the composition of the ice mantle changes over time. High activation energy reactions appear to be negligible.

2. Surface reactions on dust grains are able to increase the D/H ratio of water ice from 3.7×10^{-6} to a theoretical maximum of 1.8×10^{-5} at a distance of 60 AU from the star, increasing it by a factor of ~ 5. Although higher temperatures at distances closer to the star result in much higher reaction rates, the initial D/H ratio plays a more significant role when looking at how much it can be enhanced through surface reactions.

This implies that even at distances further out into the protoplanetary disk, the HDO/H_2O ice ratio is enhanced by surface reactions despite lower temperatures.

For future work we suggest the implementation of a chemical model into SHAMPOO, updating the adsorption energies of some deuterated species in the background model to more recent values, and investigating the r $>$ 60 AU regime of protoplanetary disks with a larger sample size.

References

Aikawa Y., Herbst E., 1999, , 351, 233

Barrière-Fouchet L., Gonzalez J. F., Murray J. R., Humble R. J., Maddison S. T., 2005, , 443, 185

Brown W. A., Bolina A. S., 2007, , 374, 1006

Caselli P., Stantcheva T., Shalabiea O., Shematovich V. I., Herbst E., 2002, , 50, 1257

Cazaux S., Tielens A. G. G. M., 2002, The Astrophysical Journal, 575, L29

Cuppen H. M., 2017,] 10.1007/s11214-016-0319-3, 212, 58

Dominik C., Tielens A. G. G. M., 1997, , 480, 647

Friedman S. D., Chayer P., Jenkins E. B., Tripp T. M., Williger G. M., Hébrard G., Sonnentrucker P., 2023, The Astrophysical Journal, 946, 34

Furuya K., Aikawa Y., Nomura H., Hersant F., Wakelam V., 2013, The Astrophysical Journal, 779, 11

Garaud P., Barrière-Fouchet L., Lin D. N. C., 2004, , 603, 292

Garrod R. T., Herbst E., 2006, , 457, 927

Garrod R. T., Widicus Weaver S. L., Herbst E., 2008, , 682, 283

Gunkelmann N., Ringl C., Urbassek H. M., 2016, , 589, A30

Haisch Karl E. J., Lada E. A., Lada C. J., 2001, , 553, L153

Kamp I., Tilling I., Woitke P., Thi W. F., Hogerheijde M., 2010, , 510, A18

LeBlanc F., 2010, An Introduction to Stellar Astrophysics

Masgrau L., González-Lafont , Lluch J. M., 1999, Journal of Computational Chemistry, 20, 1685

Öberg K. I., Bergin E. A., 2021, , 893, 1

Öberg K. I., Facchini S., Anderson D. E., 2023, , 61, 287

Oosterloo M., Kamp I., van Westrenen W., Dominik C., 2023, , 674, A124

Rocha W. R. M., Woitke P., Pilling S., Thi W. F., Jørgensen J. K., Kristensen L. E., Perotti G., Kamp I., 2023, , 673, A70

Ruffle D. P., Herbst E., 2000, , 319, 837

Ryden B., 2016, Introduction to Cosmology, 2 edn. Cambridge University Press

Siess L., Dufour E., Forestini M., 2000, , 358, 593

Stepinski T. F., Valageas P., 1996, , 309, 301

Stepinski T. F., Valageas P., 1997, , 319, 1007

Thi W. F., Woitke P., Kamp I., 2011, , 412, 711

Thi W. F., Kamp I., Woitke P., van der Plas G., Bertelsen R., Wiesenfeld L., 2013, , 551, A49

Weidenschilling S. J., 1977, , 180, 57

Whipple F. L., 1973, in Hemenway C. L., Millman P. M., Cook A. F., eds, , Vol. 319, NASA Special Publication. p. 355

Woitke P., Kamp I., Thi W. F., 2009, , 501, 383

Woitke P., et al., 2016, , 586, A103

van Dishoeck E. F., et al., 2011, , 123, 138

van Dishoeck E. F., Herbst E., Neufeld D. A., 2013, Chemical Reviews, 113, 9043